ESD-TR-89-163

Technical Report
855

Evaluation of a Delay-Doppler Imaging Algorithm Based on the Wigner-Ville Distribution

K.I. Schultz

18 October 1989

Lincoln Laboratory

MASSACHUSETTS INSTITUTE OF TECHNOLOGY

LEXINGTON, MASSACHUSETTS

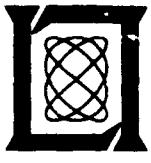

Prepared for the Department of the Navy under Air Force Contract F19628-90-C-0002.

This report is based on studies performed at Lincoln Laboratory, a center for research operated by Massachusetts Institute of Technology. The work was sponsored by the Office of Naval Research, Department of the Navy under Air Force Contract F19628-90-C-0002.

The ESD Public Affairs Office has reviewed this report, and it is releasable to the National Technical Information Service, where it will be available to the general public, including foreign nationals.

This technical report has been reviewed and is approved for publication.

FOR THE COMMANDER

Hugh L. Southall

Hugh L. Southall, Lt. Col., USAF
Chief, ESD Lincoln Laboratory Project Office

Non-Lincoln Recipients

PLEASE DO NOT RETURN

Permission is given to destroy this document when it is no longer needed.

(2)

MASSACHUSETTS INSTITUTE OF TECHNOLOGY
LINCOLN LABORATORY

EVALUATION OF A DELAY-DOPPLER IMAGING ALGORITHM BASED ON THE WIGNER-VILLE DISTRIBUTION

K.I. SCHULTZ
Group 52

TECHNICAL REPORT 855

18 OCTOBER 1989

LEXINGTON MASSACHUSETTS

ABSTRACT

This report investigates the relative merits of a delay-Doppler imaging radar based on matched filter and Wigner-Ville approaches. Both approaches are formally equivalent; the relative merits of each method are based solely on implementation issues. Given the current state of optical delay-Doppler radar and signal processing capabilities, the matched filter approach provides significant advantages over a Wigner-Ville-based approach. Additional applications of the Wigner-Ville distribution to laser radar measurements are discussed.

TABLE OF CONTENTS

LIST OF ILLUSTRATIONS

LIST OF TABLES

1. INTRODUCTION

Harper Whitehouse of NOSC proposed an alternative delay-Doppler imaging algorithm based on the Wigner-Ville distribution (WVD). Bill Miceli of the Office of Naval Research (ONR) sponsored an unconventional imaging program at Lincoln Laboratory to evaluate this technique relative to more traditional matched filter-based delay-Doppler imaging techniques. This report presents the results of this effort.

The primary purpose of this report is to evaluate the relative merits of a delay-Doppler imaging radar based on matched filter and Wigner-Ville approaches. Both approaches are formally equivalent: the relative merits of each method are based solely on implementation issues. Given an appropriate transmit waveform, the output of a practical matched filter receiver can produce a delay-Doppler image directly. In contrast, a WVD approach requires a deconvolution operation to obtain the desired delay-Doppler image. For nominal operating conditions, the matched filter approach can process data over a relatively small delay-Doppler window without sacrificing image resolution. This can significantly reduce the computational effort required to obtain an image. To maintain image resolution, a WVD approach must process data over a time-frequency window equal to the time-frequency extent of the received waveform. This requirement becomes prohibitive for high time-bandwidth product waveforms. Given the current state of optical range-Doppler radar and signal processing capabilities, the matched filter approach is preferable to a Wigner-Ville-based approach.

While the Wigner-Ville approach does not appear to be the method of choice for delay-Doppler imaging, it may be useful in other laser radar applications. Specifically, the WVD is a joint time-frequency representation of a signal which may be applied to the analysis of time-varying heterodyne or autodyne Doppler-resolved measurements of vibrating and/or rotating targets.

This report is organized as follows. The motivation, definition, basic properties, and examples of the WVD are discussed in Section 2. The relation between the Wigner-Ville and (symmetric) ambiguity function is given in Section 3. Section 4 is a discussion of the application of both the WVD and ambiguity function to delay-Doppler imaging. Conclusions and alternative applications of the Wigner-Ville distribution to optical delay-Doppler-resolved laser radar measurements are presented in Sections 5 and 6, respectively.

2. FORMULATION

2.1 BACKGROUND

Mixed time-frequency representations attempt to simultaneously analyze the energy distribution of nonstationary signals in both time and frequency. These techniques may therefore be interpreted as generalizations of Fourier analysis techniques which determine the spectral energy density of stationary signals. A simple mixed time-frequency representation which is commonly employed is the short-term Fourier transform (STFT) or spectrogram. In this technique the signal is assumed stationary over some short time interval, and standard Fourier transform techniques (e.g., FFT) are used to obtain a frequency spectrum of data within this interval. By computing spectra over successive time intervals, a time-frequency representation of the signal is obtained. In the context of laser radar measurements, this technique has been used to obtain mixed time-frequency representations of heterodyne and autodyne Doppler-resolved measurements of rotating targets.[1,2] [In the laser radar terminology, this mixed time-frequency representation has been referred to as a Doppler-time intensity (DTI) plot.] The principal shortcoming of STFT-based methods is the trade-off between frequency and time resolution. In addition, the STFT does not reproduce the energy density spectrum and the instantaneous power of a signal. A class of time-frequency representations which overcome these shortcomings has been developed.[3-5] One such representation, the Wigner-Ville distribution (WVD), was first introduced in the area of quantum mechanics by Wigner in 1932 and later into the field of communications by Ville in 1948 (References 3 and 4).

Joint time-frequency representations of a waveform have properties similar to those of joint probability density functions; these functions must be positive definite and satisfy certain zeroth-order moment or marginal requirements. Physically, these representations estimate the time-frequency energy distribution of nonstationary signals or random processes and must therefore satisfy both positivity and energy conservation constraints.[6] For a signal $x(t)$ with Fourier transform $X(\omega)$, we require that the 2-D time-frequency representation $F(t,\omega)$ have the following properties:

$$F(t,\omega) \geq 0 \quad , \quad \text{positivity} \tag{2.1}$$

$$\int F(t,\omega)d\omega = |x(t)|^2 \quad , \quad \text{instantaneous power} \tag{2.2}$$

$$\int F(t,\omega)dt = |X(\omega)|^2 \quad , \quad \text{spectral density} \tag{2.3}$$

$$\iint F(t,\omega)d\omega\, dt = \|x\|^2 \quad , \quad \text{total signal energy} \quad . \tag{2.4}$$

Integrals go from $-\infty$ to ∞ unless otherwise noted. While the WVD satisfies conditions (2.2) through (2.4) and provides additional useful information concerning the energy distribution of the function in time and

frequency, it does not, in general, satisfy the positivity condition expressed in (2.1). Cohen *et al.* have proven the existence of a class of positive time-frequency representations which satisfy conditions (2.1) through (2.4).[7] This important class of positive time-frequency distributions is not discussed here.

2.2 DEFINITION OF THE WIGNER-VILLE DISTRIBUTION

The cross WVD of two time signals x(t) and y(t) has the following bilinear form:

$$W_{x,y}(t,\omega) = \int x\left(t+\frac{\tau}{2}\right)y^*\left(t-\frac{\tau}{2}\right)e^{-j\omega\tau}d\tau \quad . \tag{2.5}$$

The auto WVD of the time function x(t) is

$$W_x(t,\omega) = W_{x,x}(t,\omega) = \int x\left(t+\frac{\tau}{2}\right)x^*\left(t-\frac{\tau}{2}\right)e^{-j\omega\tau}d\tau \quad . \tag{2.6}$$

There is a functional similarity between the above equations and the (symmetric form of the) cross ambiguity and auto ambiguity functions. The relation between the ambiguity function and WVD will be discussed in Section 3.

The WVD of $X(\omega)$ and $Y(\omega)$, the Fourier transforms of x(t) and y(t), respectively, is

$$W_{X,Y}(\omega,t) = \int X\left(\omega+\frac{\zeta}{2}\right)Y^*\left(\omega-\frac{\zeta}{2}\right)e^{-j\zeta t}d\zeta \quad . \tag{2.7}$$

It can easily be shown that

$$W_{X,Y}(\omega,t) = W_{x,y}(t,\omega) \quad . \tag{2.8}$$

In words, the cross WVD of the spectra of two signals can be computed directly from the WVD of the respective time signals simply by exchanging the frequency and time variables.

2.3 PROPERTIES OF THE WIGNER-VILLE DISTRIBUTION

A partial list of the properties of the WVD is provided below. Properties and proofs may be found elsewhere (see, for example, References 7 and 8).

2.3.1 Symmetry

$$W_{x,y}(t,\omega) = W^*_{y,x}(t,\omega) \Rightarrow W_x(t,\omega) = W^*_x(t,\omega) \quad . \tag{2.9}$$

The WVD of any real or complex function is real.

2.3.2 Time shifts

A time shift in both time signals results in an identical time shift in the cross WVD.

2.3.3 Modulation

Modulating each time signal by $\exp(j\Omega t)$ results in a frequency shift of the resultant cross WVD by Ω.

2.3.4 WVD for Time-Limited Signals

If the time signals x(t) and y(t) are restricted to a finite time interval, then the cross-WVD distribution is restricted to the identical time interval for all frequencies.

2.3.5 WVD for Frequency-Limited Signals

If the spectra of signals x(t) and y(t) are band-limited, then the cross-WVD distribution will be similarly band-limited.

2.3.6 Nonlinearity

The WVD is a bilinear function of two signals; the WVD of the algebraic sum of two signals is not the algebraic sum of the WVD of each signal.

$$W_{x+y}(t,\omega) = W_x(t,\omega) + W_y(t,\omega) + 2\,\mathrm{Re}\left[W_{x,y}(t,\omega)\right] \quad . \tag{2.10}$$

The third term in Equation (2.10) represents the cross or interference term and is the result of the (second order) nonlinear form of the WVD. The interference term may pose a problem in the analysis of multicomponent signals.[9,10] By low-pass filtering the WVD, one may reduce the interference effects by sacrificing resolution. This issue is similar to the sidelobe-resolution trade-off in standard Fourier analysis.

2.3.7 Marginal Relations (Zeroth-Order Moments)

For the cross WVD we have

$$\frac{1}{2\pi}\int W_{x,y}(t,\omega)\,d\omega = x(t)g^*(t) \quad , \tag{2.11}$$

$$\int W_{x,y}(t,\omega)\,dt = X(\omega)Y^*(\omega) \quad ; \tag{2.12}$$

which reduce to the following expressions for the auto WVD

$$\frac{1}{2\pi}\int W_x(t,\omega)\,d\omega = |x(t)|^2 \quad , \tag{2.13}$$

$$\int W_x(t,\omega)\,dt = |X(\omega)|^2 \quad . \tag{2.14}$$

Finally the total energy in x(t) is given by the integral of the auto WVD over the entire time-frequency plane

$$\frac{1}{2\pi}\iint W_x(t,\omega)\,dt\,d\omega = \int |x(t)|^2 dt = \|x\|^2 \quad . \tag{2.15}$$

2.3.8 First-Order Moments

The marginal relations presented in Section 2.3.7 are zeroth-order moment expressions. Here, we consider first-order moments of the WVD in both time and frequency. The WVD has the useful property that the first-order moments in time and frequency are the signal instantaneous frequency and group delay, respectively.

An expression for $\Omega_x(t)$, the average frequency of the WVD as a function of time, is given by the following expression

$$\Omega_x(t) = \frac{\int \omega W_x(t,\omega)\,d\omega}{\int W_x(t,\omega)\,d\omega} \quad . \tag{2.16}$$

which simplifies to[8]

$$\Omega_x(t) = \mathrm{Im}\left[\frac{x'(t)}{x(t)}\right] \quad . \tag{2.17}$$

Here, Im [*] is the imaginary-part operation and the prime (') denotes differentiation. This expression is identically zero for real valued functions. Let x(t) be a complex analytic signal which can be expressed as follows

$$x(t) = a(t)e^{j\phi(t)} \quad , \tag{2.18}$$

with a(t) and $\phi(t)$ real functions of time. The average frequency of the WVD for such a function is given by

$$\Omega_x(t) = \phi'(t) \quad . \tag{2.19}$$

The average frequency of the WVD at time t is equal to the instantaneous frequency of the complex analytic signal.

An expression for $T_x(\omega)$, the average time of the WVD as a function of frequency, is given by the following expression

$$T_x(\omega) = \frac{\int t W_x(t,\omega)\,dt}{\int W_x(t,\omega)\,dt} \quad . \tag{2.20}$$

which simplifies as follows[8]

$$T_x(\omega) = -\mathrm{Im}\left[\frac{X'(\omega)}{X(\omega)}\right] \quad . \tag{2.21}$$

Here, $X(\omega)$ is the Fourier transform of the time signal $x(t)$, Im [*] takes the imaginary part of the operand, and the prime denotes differentiation. This expression is identically zero for real valued functions. Let $X(\omega)$ be a complex analytic signal which can be expressed as follows

$$X(\omega) = \alpha(\omega)e^{j\theta(\omega)} \quad , \tag{2.22}$$

with $\alpha(\omega)$ and $\theta(\omega)$ real functions of frequency. The average frequency of the WVD for such a function is given by

$$T_x(\omega) = -\theta'(\omega) \quad . \tag{2.23}$$

The time average of the WVD at a given frequency is equal to the signal group delay.

2.3.9 Second-Order Moments

Local second-order moments in time and frequency (defined in the usual way) are a measure of the spread of the WVD about mean time or frequency values, respectively. As the WVD is not positive definite, the local second-order moments of the WVD distribution may be negative, a result which is inconsistent with a strict probability theory interpretation. However, these moments may still provide useful information; as second-order moments tend to characterize structural features in the WVD, they may be used to indicate the structure of multicomponent signals.[10]

2.4 ANALYTIC SIGNAL REQUIREMENT

For (complex) analytic signals, the first-order moments of the WVD in time and frequency are the *instantaneous frequency and group delay*, respectively. Strictly speaking, these properties do not apply to real valued signals. In particular, if we let the signal $r(t)$ represent the real part of an analytic signal $x(t)$, then

$$W_r(t,\omega) = \frac{1}{4}\left[W_x(t,\omega) + W_x(t,-\omega)\right] + g(t,\omega) \quad , \tag{2.24}$$

where

$W_r(t,\omega)$ = WVD of the real signal $r(t)$

$W_x(t,\omega)$ = WVD of the analytic signal $x(t)$

$g(t,\omega)$ = oscillatory fringe pattern.

The WVD of a real signal, as depicted in Figure 1(b), is composed of three terms, the desired "image" term $W_x(t,\omega)$, a conjugate image term $W_x(t,-\omega)$, and a residual low-frequency fringe pattern $g(t,\omega)$. Analysis has shown that the artifacts embodied in the $g(t,\omega)$ term have no physical meaning (see, for example, Reference 9). The analytic signal requirement must be taken into consideration when implementing the WVD.

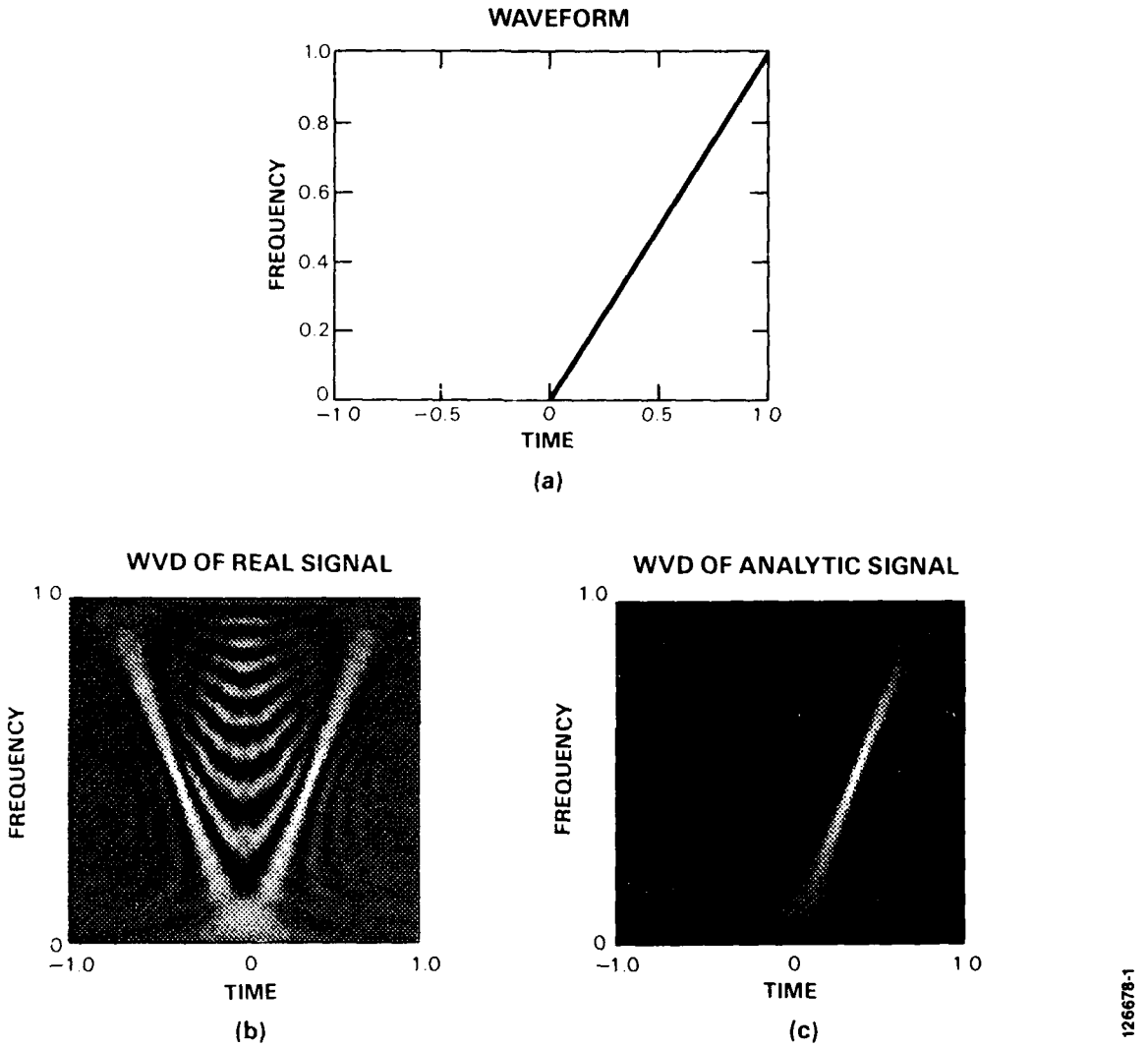

Figure 1. Analytic signal requirement. The time-frequency character of a linear chirp signal is given in (a). Both the time and frequency axes have been normalized to unit time and frequency, respectively. The WVD of a real signal with time-frequency characteristics given in (a) is shown in (b). The WVD is characterized by the image, conjugate image, and residual fringe pattern components. The WVD of the analytic linear FM chirp is shown in (c). The frequency time characteristics of the signal are clearly reproduced in the WVD.

2.5 MULTICOMPONENT SIGNALS

Laser radar measurements of complex targets are generally characterized by complicated multicomponent signals. The WVD of a multicomponent signal is complicated, however, by two factors: (1) negative second-order moments, and (2) the presence of interference terms (which are manifest as oscillatory fringe patterns in the WVD — see Section 2.3.6). Both these effects may be reduced, at the expense of resolution, by low-pass filtering the WVD.[9] Time-frequency distributions have been proposed which either eliminate or suppress the undesirable properties of the WVD.[5,10]

2.6 EXAMPLES

In this section we demonstrate the basic properties of the WVD by example. We begin by considering the WVD of a simple up-chirp waveform, as shown in Figure 1(a). The WVD of the up chirp is shown in Figure 2(a). The time-frequency characteristics of the up chirp are clearly manifest in the WVD. The first-order moment in frequency, which is the instantaneous frequency estimate, is shown in Figure 2(b). Note that the spread or variance about the true instantaneous frequency is varying but bounded. It is interesting to note that the local variance of the WVD tends to increase at discontinuities in the underlying instantaneous frequency of the signal.

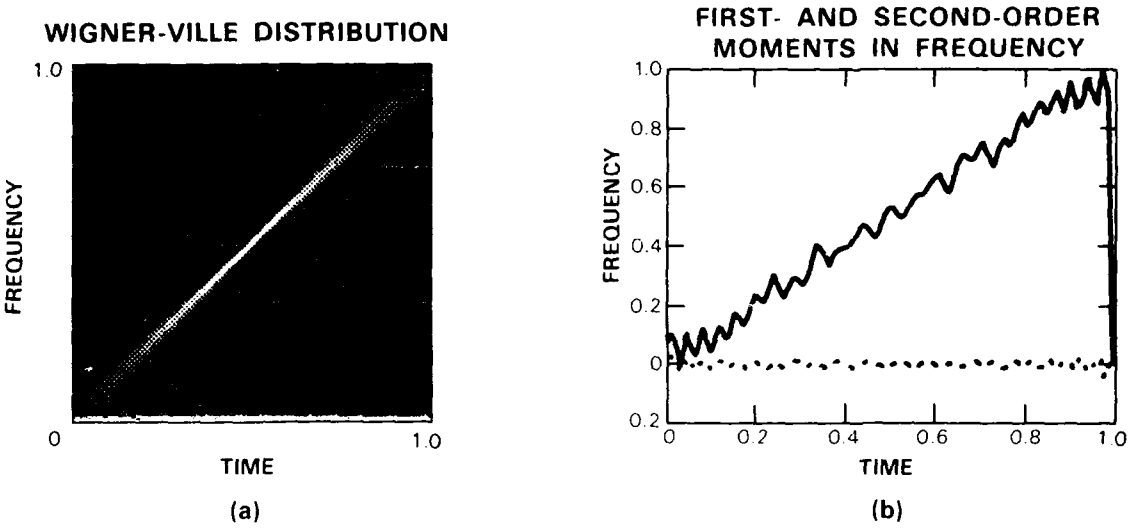

126678-2

Figure 2. The WVD and local moments of a single up chirp. The WVD of the analytic up chirp is shown in (a). Normalized time-frequency axes are used. The first- and second-order moments of the WVD are shown in (b) as the solid and dashed lines, respectively. The mean represents a reasonable estimate of the instantaneous frequency of the analytic up-chirp waveform. The variance is reasonably uniform and small, indicating that the "knife-edge" ridge defining the chirp in (a) is well defined.

The WVDs for different multicomponent up-down chirp signals are shown in Figures 3 through 5. The undesirable oscillatory fringe pattern in these figures is the result of the bilinear form of the WVD; the WVD of the composite up-down chirp is not equal to the sum of the WVD of each constituent chirp. Due to the oscillatory nature of the cross-term component, this term may be reduced by low-pass filtering the WVD.

2.7 IMPLEMENTATION

Although computational complexity is inherent in an algorithm which generates a 2-D distribution from 1-D data, implementation issues are not addressed in this report. Efficient numerical algorithms may be found in the literature.[11,12] Optical implementation of the WVD is also a current topic of investigation.[13-16]

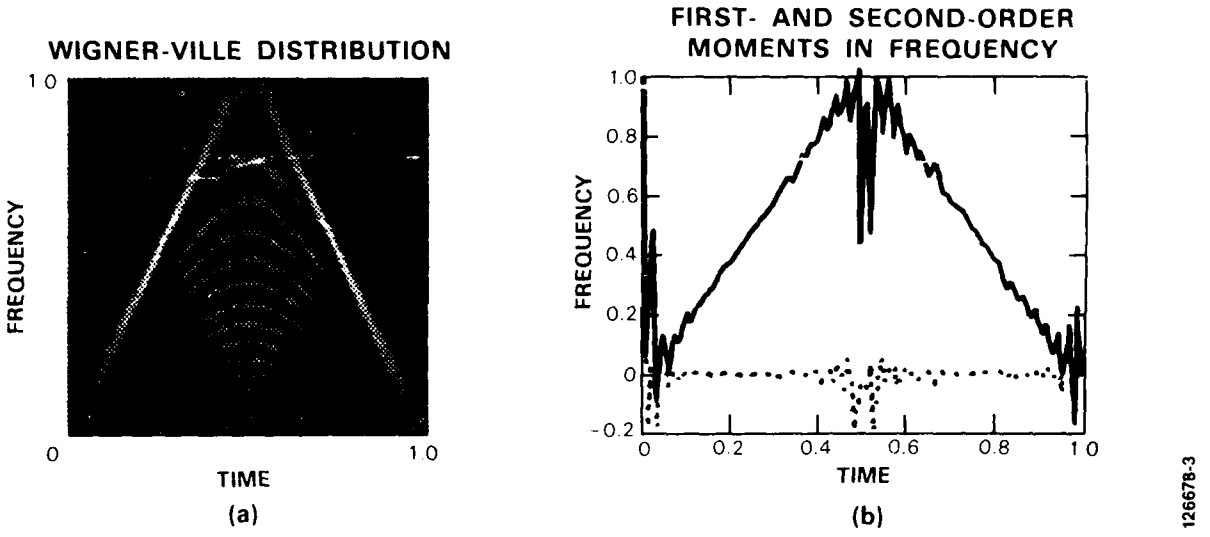

Figure 3. The WVD and local moments of an up-down chirp waveform. Normalized time-frequency axes are used. In this example, the chirps have the same frequency bandwidth and time duration. The WVD of the (analytic) up-down chirp is shown in (a). The fringe pattern is due to the (second order) nonlinearity of the WVD. The first- and second-order moments of the WVD are shown in (b) as the solid and dashed lines, respectively. The mean represents a reasonable estimate of the instantaneous frequency of the analytic up-chirp waveform.

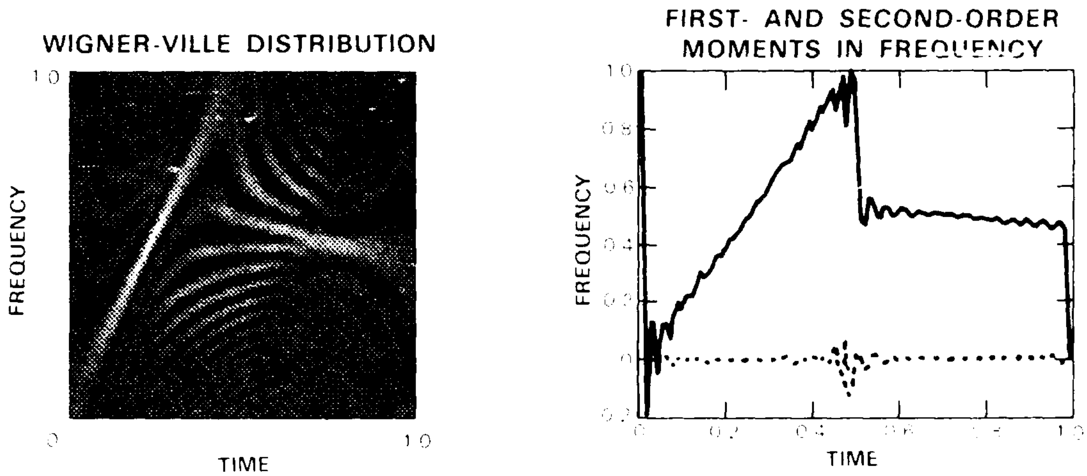

(a) (b)

126678-4

Figure 4. The WVD [illegible]

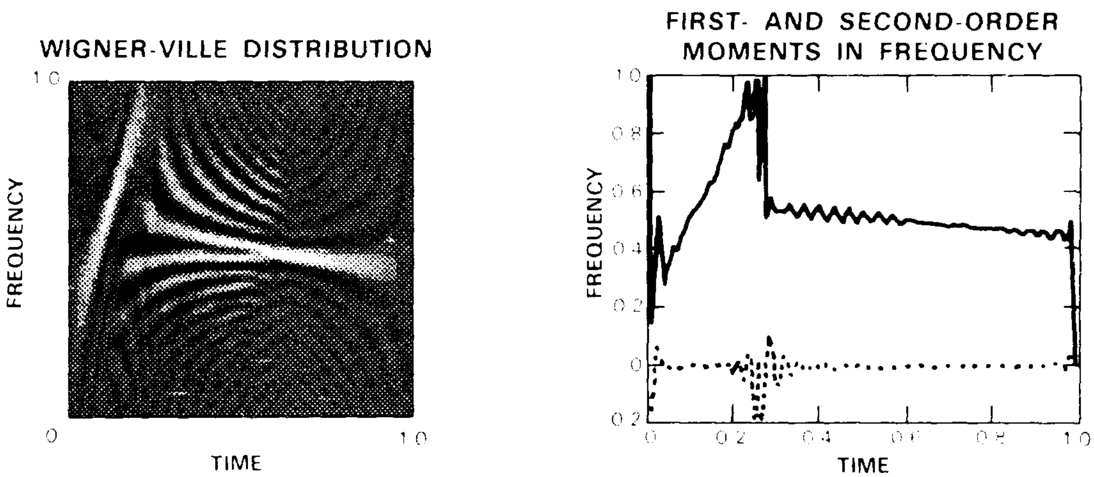

(a) (b)

126678-5

Figure 5. The WVD [illegible]

3. RELATION BETWEEN THE WIGNER-VILLE DISTRIBUTION AND THE AMBIGUITY FUNCTION

Both the WVD and the ambiguity function (AF) are mixed 2-D representations of a 1-D signal. The utility of the WVD as a time-frequency analysis tool, along with a partial list of applications to optical radar, has been discussed. In the context of optical radar, the AF is a useful tool to evaluate the performance of a 2-D delay-Doppler matched filter receiver. In this case, the magnitude squared of the ambiguity function may be interpreted as the point spread response of a delay-Doppler imaging system.

For a given signal x(t), the WVD $W_x(t,\omega)$ and the ambiguity function $A_x(\zeta,\tau)$ are defined as follows:

$$W_x(t,\omega) = \int x\left(t+\frac{\tau}{2}\right)x^*\left(t-\frac{\tau}{2}\right)e^{-j\tau\omega}d\tau \quad , \tag{3.1}$$

$$A_x(\zeta,\tau) = \int x\left(t+\frac{\tau}{2}\right)x^*\left(t-\frac{\tau}{2}\right)e^{-jt\zeta}dt \quad . \tag{3.2}$$

These equations imply that the AF and WVD form a Fourier-transform pair [17-19]

$$A_x(\zeta,\tau) = \mathbf{F}W_x(t,\omega) \quad , \tag{3.3}$$

$$W_x(t,\omega) = \mathbf{F}^{-1}A_x(\zeta,\tau) \quad , \tag{3.4}$$

where **F** and $\mathbf{F}^{-1}$ are the Fourier-transform operations defined as follows

$$\mathbf{F} = \frac{1}{2\pi}\iint e^{-j(\zeta t-\omega\tau)}d\tau\,d\zeta \quad , \tag{3.5}$$

$$\mathbf{F}^{-1} = \iint e^{j(\zeta t-\omega\tau)}dt\,d\omega \quad . \tag{3.6}$$

The Wigner-Ville distribution and ambiguity function are two different representations of the same data. A comparison of the effect of certain signal operations on the WVD and AF are listed in Table I. Note that time and frequency shifts of the original signal are preserved in the WVD representation, but are mapped into a complex oscillation in the AF representation. Assuming that both the WVD and AF have similar hardware (or software) implementations, the decision to use one method over another depends entirely on which method provides the most satisfactory data representation for a given application.

Figure 6 illustrates the ambiguity diagram and WVD for an up-down chirp waveform. The forward Fourier transform of the product $x(t+\tau/2)\,x^*(t-\tau/2)$ with respect to delay τ results in the WVD, while the forward Fourier transform of the product $x(t+\tau/2)\,x^*(t-\tau/2)$ with respect to time produces the AF. (The ambiguity diagram shown is the magnitude of the AF.) The 2-D Fourier relation is clear: the inverse Fourier

TABLE I (Reference 8)

Properties of the Wigner-Ville Distribution (WVD) and the Ambiguity Function (AF)

	Signal	Spectrum	WVD	AF
Original	$x(t)$	$X(\omega)$	$W_x(t,\omega)$	$A_x(\zeta,\tau)$
Data Type	Complex	Complex	Real	Complex
Time Shift	$x(t-t_0)$	$X(w)\, e^{-j\omega t_0}$	$W_x(t-t_0,\omega)$	$A_x(\zeta,\tau)\, e^{j\zeta t_0}$
Frequency Shift	$x(t)\, e^{j\omega t_0}$	$X(\omega-\omega_0)$	$W_x(t,\omega-\omega_0)$	$A_x(\zeta,\tau)\, e^{j\omega_0\tau}$
Filtering	$\int x(u)\, h(t-u)\, du$	$x(\omega)\, H(\omega)$	$\int W_x(u,\omega)\, W_h(t-u,\omega)\, du$	$\int A_x(\zeta,u)\, A_h(\zeta,\tau-u)\, du$
Modulation	$x(t)\, m(t)$	$\frac{1}{2\pi}\int X(v)\, M(\omega - v)\, dv$	$\frac{1}{2\pi}\int W_x(t,v)\, W_m(t,\omega - v)\, dv$	$\frac{1}{2\pi}\int A_x(v,\tau)\, A_m(\zeta - v,\tau)\, dv$

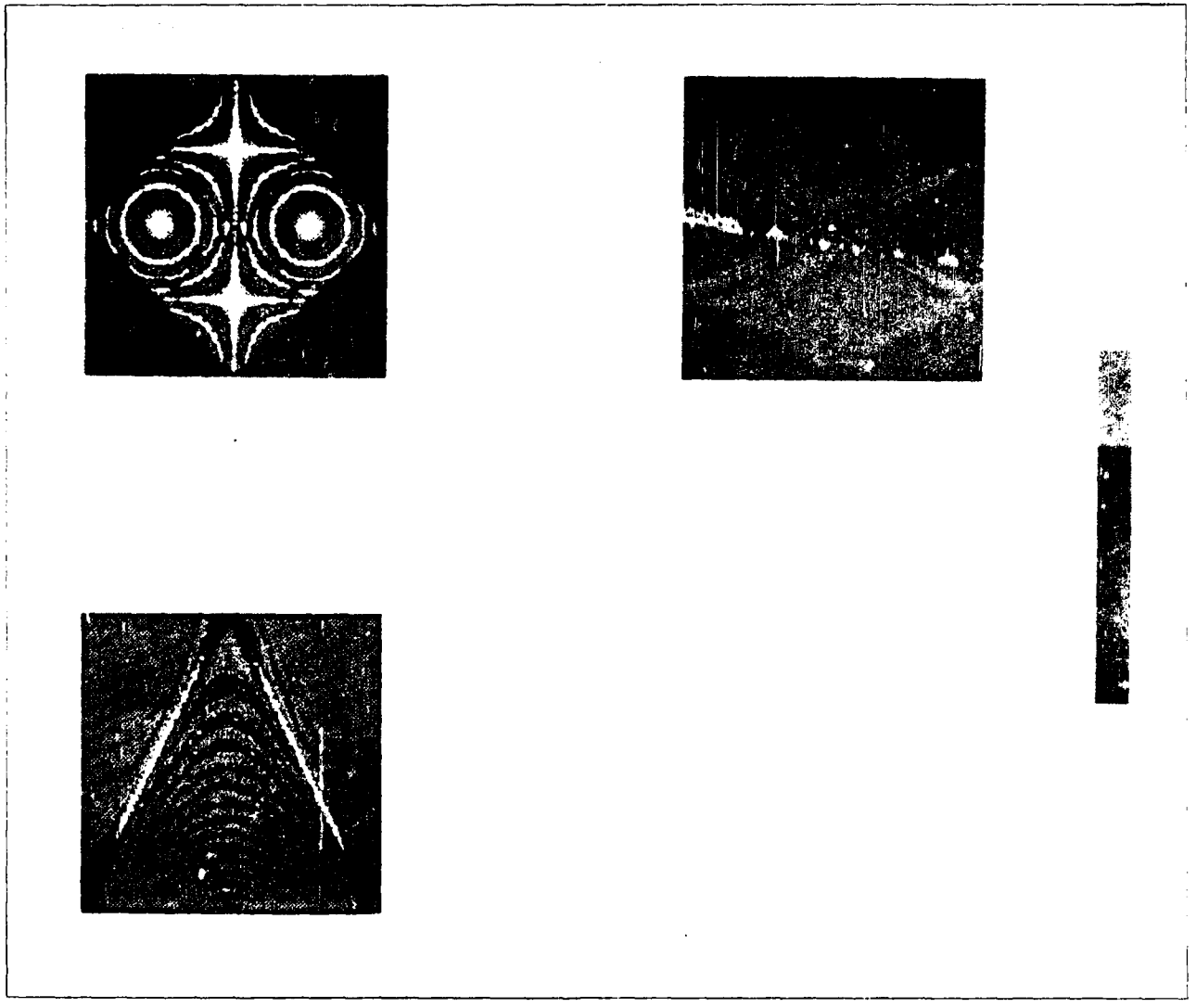

transform of the WVD with respect to delay followed by a forward Fourier transform with respect to time produces the AF. Note that time-frequency characteristics of the original up-down chirp waveform are clearly evident in the WVD. The fringe patterns evident in the WVD are the so-called cross-terms or interference terms, and are the consequence of the bilinear form of the WVD kernel. The ambiguity diagram of the up-down chirp is characterized by a central peak plus relatively high sidelobes which represent the "ambiguity" of each chirp. Due to the Fourier relation between the AF and WVD, the AF becomes more localized in the delay-Doppler plane and the corresponding WVD becomes increasingly distributed throughout the time-frequency plane. This is an important result in the context of delay-Doppler imaging.

4. DELAY-DOPPLER IMAGING

4.1 CONVENTIONAL MATCHED FILTER APPROACH

In the conventional analysis of delay-Doppler imaging, the output of a 2-D delay-Doppler matched filter represents the convolution of an underlying target distribution in delay-Doppler space, denoted by $\sigma(\zeta,\tau)$ convolved with the magnitude squared of the ambiguity function or point spread response (PSR) of the filter. Unlike conventional spatial imaging systems whose PSR depends on a spatial aperture, the PSR of the delay-Doppler imaging system is determined by the time-frequency properties of the transmitted waveform. If, for example, one could generate a thumbtack-like PSR, the output of the 2-D matched filter would represent the 2-D delay-Doppler image of the target. The relation between the output of a 2-D matched filter and the underlying delay-Doppler distribution of the target is given by the following expression:[20]

$$\left\langle \left| A_{x,y}(\zeta,\tau) \right|^2 \right\rangle = \iint \sigma(\zeta',\tau') \left| A_x[\zeta-(\zeta'-\zeta_0),\tau-(\tau'-\tau_0))] \right|^2 d\tau' d\zeta' \quad , \tag{4.1}$$

where

$x(t)$	=	transmitted waveform
$y(t)$	=	received waveform
$\sigma(\zeta,\tau)$	=	target cross-section distribution in delay and Doppler
$A_x(\zeta,\tau)$	=	auto ambiguity function of transmitted waveform
$A_{x,y}(\zeta,\tau)$	=	cross ambiguity function of received and transmitted waveforms
τ_0	=	filter mismatch in delay (tracking error)
ζ_0	=	filter mismatch in Doppler (tracking error).

Here, the operator <> indicates an ensemble average (e.g., an average over different speckle realizations). The basic assumptions used to derive Equation (4.1) may be found in Rihaczek.[20] The output of the 2-D matched filter is the cross ambiguity function between the transmitted and received waveforms. As the filter output $<|A_{x,y}(\zeta,\tau)|^2>$ represents the convolution between the desired target cross-section distribution $\sigma(\zeta,\tau)$ with the magnitude squared auto ambiguity function $|A_x(\zeta,\tau)|^2$ of the transmitted waveform, $|A_x(\zeta,\tau)|^2$ may be interpreted as the PSR of a delay-Doppler imaging system.

Given flexibility in waveform generation and reception, one could select a waveform with a thumbtack-like ambiguity function resulting in a matched filter output which approximates the underlying target cross-section distribution; there is no need to invert Equation (4.1) for $\sigma(\zeta,\tau)$.

4.2 WIGNER-VILLE APPROACH

Harper Whitehouse derived a delay-Doppler imaging technique based on the WVD.[21] The starting point is Equation (4.1). Substituting the following two relations[19,22,25]

$$\mathbf{F}\left| A_{x,y}(\zeta,\tau) \right|^2 = A_x^*(\zeta,\tau)\, A_y(\zeta,\tau) \tag{4.2}$$

and

$$\mathbf{F}^{-1}A_x(\zeta,\tau) = W_x(t,\omega) \tag{4.3}$$

into Equation (4.1) gives the following result

$$\left\langle W_y(t,\omega)\right\rangle = \iint \sigma(t',\omega')\, W_x(t-t',\omega-\omega')\,d\omega'dt' \quad . \tag{4.4}$$

This expression is the basis for delay-Doppler imaging with the WVD. It states that the expectation of the WVD of the received waveform is equal to the convolution of the underlying delay-Doppler target cross section with the WVD of the transmitted signal. Note that (1) a cross-WVD computation is not required, (2) the WVD of the transmit signal may be interpreted as the PSR of the WVD-based imaging system, and (3) the matched filter and Wigner-Ville imaging systems [as defined by Equations (4.1) and (4.4), respectively] are different representations of the same underlying process; from an information theoretic point of view, the methods are identical.

4.3 COMPARISON OF THE MATCHED FILTER AND WIGNER-VILLE APPROACHES

As previously stated, the matched filter and Wigner-Ville approaches are equivalent from a theoretical viewpoint. Imaging with the two approaches is, however, very different. The comparison of the matched filter and Wigner-Ville-based delay-Doppler imaging systems will begin with an evaluation of the point spread response (PSR). The PSR is a fundamental property of an imaging system. The computational requirements for each system will then be discussed. Bistatic issues will be addressed. As will become evident, S/N issues are secondary and will not be discussed here. A preliminary S/N analysis of the WVD may be found in References 23 and 24.

4.3.1 Point Spread Response

Thumbtack-like ambiguity responses for the matched filter receiver were discussed briefly in Section 4.1. In the case of waveforms which have thumbtack-like ambiguity functions (in the region of interest), delay (range) resolution is inversely proportional to the frequency bandwidth, and Doppler resolution is inversely proportional to the temporal duration of the waveform. Increasing the time-bandwidth product of these waveforms allows one to extract an increasing amount of information from the target. The time-bandwidth product of a signal may be increased by phase or frequency-modulation techniques. These techniques generally lead to simple implementations relative to those obtained using amplitude-modulation techniques. The main point is that it is possible to simultaneously obtain high resolution in both delay and Doppler by choosing a waveform with a thumbtack-like ambiguity function.

The WVD-based receiver has significantly different behavior. As shown in Equation (4.4), the PSR of a WVD-based receiver is given by the WVD of the transmit waveform. A thumbtack-like WVD requires the transmit signal to be (1) nonzero over a time interval small compared with the target extent in time, and (2) nonzero over a frequency interval small compared with the frequency extent of the target. These two conditions are generally mutually exclusive: a thumbtack-like WVD may be unrealizable for many targets

of interest. To obtain a high-resolution delay-Doppler image directly, the WVD approach requires narrowband short-duration waveforms, while the matched filter approach requires wideband long-duration waveforms. As wideband long-duration waveforms are physically realizable, the matched filter approach has a significant advantage over the WVD approach. This property is consistent with the Fourier-transform relation between the two methods: an AF which is highly localized transforms into a WVD which is highly distributed. This is demonstrated for an up-down chirp in Figure 6.

4.3.2 Computational Requirements

We begin by assuming the existence of waveforms with thumbtack-like ambiguity functions. While the computations involved in computing the full matched filter output and WVD output are identical, the output of the matched filter gives the desired image directly whereas the WVD-based method requires a deconvolution to obtain the image $\sigma(\zeta,\tau)$. This is generally an ill-posed and computationally intensive operation.

If we further assume that both the delay-Doppler tracking errors and the target cross-section delay-Doppler distribution are both small compared with the delay-Doppler extents of the waveform, then the computational requirements of the matched filter approach can be reduced significantly by limiting data processing to a relatively small delay-Doppler window. This can be done without loss of image resolution. From a practical standpoint, the time-bandwidth capacity of the signal processor may be reduced without sacrificing image resolution. In order to maintain image resolution using the WVD approach, data must be processed over time-frequency extents defined by the received waveform. As a waveform with a time-bandwidth product equal to TB has a 2-D WVD with $(TB)^2$ independent resolution cells, large TB product waveforms could prohibit real-time computation of the WVD.

4.3.3 Bistatic Considerations

It has been suggested that the WVD approach may have some advantages in a bistatic situation as the WVD receiver produces the auto WVD of the received waveform: the image is obtained after deconvolving the *auto WVD* of the received waveform with the (stored) auto WVD of the transmit waveform. In this case, a reference waveform generator is not required. This reasoning is somewhat misleading: the transmit waveform could be "stored" in a programmable matched filter or, if the receive and transmit waveforms could be digitized, a completely flexible matched filter could be implemented digitally. While these issues are technology driven, it does not appear that the WVD approach would provide significant advantages over a matched filter approach in the case of bistatic measurements.

5. CONCLUSIONS

The primary purpose of this report is to evaluate the relative merits of a delay-Doppler imaging radar based on matched filter and Wigner-Ville approaches. Both approaches are formally equivalent; the relative merits of each method are based solely on implementation issues. Given an appropriate transmit waveform, the output of a practical matched filter receiver can produce a delay-Doppler image directly. In contrast, a WVD approach requires a deconvolution operation to obtain the desired delay-Doppler image. For nominal operating conditions, the matched filter approach can process data over a relatively small delay-Doppler window without sacrificing image resolution. This can significantly reduce the computational effort required to obtain an image. To maintain image resolution, a WVD approach must process data over a time-frequency window equal to the time-frequency extent of the received waveform. This requirement becomes prohibitive for high time-bandwidth product waveforms. Given the current state of optical range-Doppler radar and signal processing capabilities, the matched filter approach is preferable to a Wigner-Ville-based approach.

6. FUTURE WORK

In optical radar applications, time-frequency representations have been used to process both heterodyne and autodyne Doppler-resolved cross-section measurements of rotating and/or vibrating targets. In particular, the short-term Fourier transform (STFT) has been used to analyze the time-frequency distribution of both autodyne and heterodyne laser radar measurements of rotating targets. Standard frequency discrimination techniques have been applied to the analysis of laser radar Doppler-resolved data of vibrating targets. An investigation into the relative merits of standard time-frequency analysis techniques (e.g., STFT, frequency discriminator, etc.) vs signal analysis using time-frequency distribution techniques (e.g., the WVD) may prove useful in these applications.

REFERENCES

1. K. Schultz, "Application of Reconstruction from Projection Techniques to Time Varying Autodyne Signatures," in *Laser Radar III*, SPIE **999**, 216-224 (1988).

2. R. Marino *et al.*, "Tomographic Imaging with Laser Radar Reflective Projections," in *Laser Radar III*, SPIE **999**, 248-268 (1988).

3. E. Wigner, Phys. Rev. **40**, 749 (1932).

4. J. Ville, Cables Trans. **2**, 61 (1948).

5. L. Cohen and T. Posch, IEEE Trans. Acoust. Speech Signal Process. **ASSP-33**, 31 (1985).

6. W. Martin and P. Flandrin, IEEE Trans. Acoust. Speech Signal Process. **ASSP-33**, 1461 (1985).

7. L. Cohen, "Properties of the Positive Time-Frequency Distribution Functions," Proc. IEEE ICASSP '85 (Cat. No. 85CH2118-8), Vol. 2, (1985), pp. 548-551.

8. T.A. Claasen and W.F. Mecklenbrauker, Philips J. Res. **35**, 217 (1980).

9. B. Boashash, "Time-Frequency Analysis and Synthesis," in *Advanced Algorithms and Architectures for Signal Processing III*, SPIE **975**, 164-185 (1988).

10. L. Cohen and C. Lee, "Instantaneous Frequency, Its Standard Deviation and Multicomponent Signals," in *Advanced Algorithms and Architectures for Signal Processing III*, SPIE **975**, 186-208 (1988).

11. B. Boashash, P. Black, and H. Whitehouse, "An Efficient Implementation for Real Time Applications of the Wigner Ville Distribution," in *Real Time Signal Processing IX*, SPIE **698**, 22-33 (1986).

12. T.A. Claasen and W.F. Mecklenbrauker, Philips J. Res. **35**, 276 (1980).

13. H. Szu, Opt. Eng. **21**, 804 (1982).

14. H. Bartlet, Opt. Commun. **32**, 32 (1980).

15. G. Eichmann and B. Dong, Appl. Opt. **21**, 3152 (1982).

16. A. Rakes, C. Hester, R. Inguva, and B. Kumar, "Wigner Distribution Function/Ambiguity Function Processor," in *Advances in Optical Information Processing III*, SPIE **936**, 260-269 (1988).

17. L. Cohen, "Generalized Ambiguity Functions," Proc. IEEE ICASSP '85 (Cat. No. 85CH2118-8), Vol. 3 (1985), pp. 1033-1036.

18. T.A. Claasen and W.F. Mecklenbrauker, Philips J. Res. **35**, 372 (1980).

19. H. Szu and J. Blodgett, "Wigner Distribution and Ambiguity Function," in *Optics in Four Dimensions-1980*, M.A. Machado and L.M. Narducci, American Institute of Physics Conference Proceedings **65**, No. 1 (1981), p. 355.

20. A. Rihaczek, *Principles of High-Resolution Radar* (Peninsula Publishing, Los Altos, California, 1985), p. 337.

21. H. Whitehouse, "Interpretation of Radar Imaging in Terms of the Wigner-Ville Distribution," in *Advanced Algorithms and Architectures for Signal Processing III*, SPIE **975**, presentation only (1988).

22. C. Stutt, "The Application of Time/Frequency Correlation Functions to the Continuous-Waveform Encoding of Message Symbols," Report No. 61-RL-2761E, General Electric Research Laboratory, Schenectady, New York (1961).

23. B. Kumar and C. Carrol, Appl. Opt. **23**, 4090 (1984).

24. B. Boashash and P. O'Shea, "Application of the Wigner-Ville Distribution to the Identification of Machine Noise," in *Aavanced Algorithms and Architectures for Signal Processing III*, SPIE **975**, 209-220 (1988).

25. H.E. VanBrundt, private communication.

REPORT DOCUMENTATION PAGE

1a. REPORT SECURITY CLASSIFICATION Unclassified	1b. RESTRICTIVE MARKINGS
2a. SECURITY CLASSIFICATION AUTHORITY	3. DISTRIBUTION/AVAILABILITY OF REPORT Approved for public release; distribution is unlimited.
2b. DECLASSIFICATION/DOWNGRADING SCHEDULE	
4. PERFORMING ORGANIZATION REPORT NUMBER(S) Technical Report 855	5. MONITORING ORGANIZATION REPORT NUMBER(S) ESD-TR-89-163
6a. NAME OF PERFORMING ORGANIZATION Lincoln Laboratory, MIT 6b. OFFICE SYMBOL *(If applicable)*	7a. NAME OF MONITORING ORGANIZATION Electronic Systems Division
6c. ADDRESS *(City, State, and Zip Code)* P.O. Box 73 Lexington, MA 02173-9108	7b. ADDRESS *(City, State, and Zip Code)* Hanscom AFB, MA 01731
8a. NAME OF FUNDING/SPONSORING ORGANIZATION Office of Naval Research 8b. OFFICE SYMBOL *(If applicable)*	9. PROCUREMENT INSTRUMENT IDENTIFICATION NUMBER F19628-90-C-0002
8c. ADDRESS *(City, State, and Zip Code)* 495 Summer Street Boston, MA 02210-2109	10. SOURCE OF FUNDING NUMBERS PROGRAM ELEMENT NO. 61102F; PROJECT NO. 272; TASK NO.; WORK UNIT ACCESSION NO

11. TITLE *(Include Security Classification)*
Evaluation of a Delay-Doppler Imaging Algorithm Based on the Wigner-Ville Distribution

12. PERSONAL AUTHOR(S)
Kenneth I. Schultz

13a. TYPE OF REPORT	13b. TIME COVERED	14. DATE OF REPORT *(Year, Month, Day)*	15. PAGE COUNT
Technical Report	FROM _____ TO _____	1989, October, 18	36

16. SUPPLEMENTARY NOTATION
None

17. COSATI CODES			18. SUBJECT TERMS *(Continue on reverse if necessary and identify by block number)*
FIELD	GROUP	SUB-GROUP	delay-Doppler imaging; Wigner-Ville distribution; laser radar measurements; matched filter; ambiguity function

19. ABSTRACT *(Continue on reverse if necessary and identify by block number)*

This report investigates the relative merits of a delay-Doppler imaging radar based on matched filter and Wigner-Ville approaches. Both approaches are formally equivalent; the relative merits of each method are based solely on implementation issues. Given the current state of optical delay-Doppler radar and signal processing capabilities, the matched filter approach provides significant advantages over a Wigner-Ville-based approach. Additional applications of the Wigner-Ville distribution to laser radar measurements are discussed.

20. DISTRIBUTION/AVAILABILITY OF ABSTRACT	21. ABSTRACT SECURITY CLASSIFICATION	
☐ UNCLASSIFIED/UNLIMITED ☒ SAME AS RPT. ☐ DTIC USERS	Unclassified	
22a. NAME OF RESPONSIBLE INDIVIDUAL Lt. Col. Hugh L. Southall, USAF	22b. TELEPHONE *(Include Area Code)* (617) 981-2330	22c. OFFICE SYMBOL ESD/TML